Simultaneous multislice diffusion-weighted imaging of the kidney: a systematic analysis of image quality

Kenkel, David ; Barth, Borna K ; Piccirelli, Marco ; Filli, Lukas ; Finkenstädt, Tim ; Reiner, Cäcilia S ; Boss, Andreas

Abstract: OBJECTIVES The aims of this study were to implement a protocol for simultaneous multislice (SMS) accelerated diffusion-weighted imaging (DWI) of the kidneys and to perform a systematic analysis of image quality of the data sets. MATERIALS AND METHODS Ten healthy subjects and 5 patients with renal masses underwent DWI of the kidney in this prospective institutional review board-approved study on a 3 T magnetic resonance scanner. Simultaneous multislice DWI echo-planar sequences (acceleration factors [AFs] 2 and 3) were compared with conventional echo-planar DWI as reference standard for each acquisition scheme. The following 3 acquisition schemes were applied: comparison A, with increased number of acquisitions at constant scan time; comparison B, with reduction of acquisition time; and comparison C, with increased slice resolution (constant acquisition time, increasing number of slices). Interreader reliability was analyzed by calculating the intraclass correlation coefficient (ICC). Qualitative image quality features were evaluated by 2 independent radiologists on a 5-point Likert scale. Quantification accuracy of the apparent diffusion coefficients (ADCs) and signal-to-noise ratios (SNRs) were assessed by region of interest analysis. Furthermore, lesion conspicuity in the 5 patients was assessed using a 5-point Likert scale by 2 independent radiologists. RESULTS Interreader agreement was substantial with an ICC of 0.68 for the overall image quality and an ICC of 0.73 for the analysis of artifacts. In comparison A, AF2 resulted in increased SNR ($P < 0.05$) by 21% at stable image quality scores (image quality: $P = 0.76$, artifacts: $P = 0.21$). In comparison B, applying AF2, the scan time could be reduced by 46% without significant reduction in qualitative image quality scores ($P = 0.059$) or SNR ($P = 0.126$). In comparison C, slice resolution could be improved by 28% using AF2 with stable image quality scores and SNR. In general, AF3 resulted in reduced image quality and SNR. Significantly reduced ADC values were observed for AF3 in comparison C (cortex: $P = 0.003$; medulla: $P = 0.001$) compared with the standard echo-planar imaging sequence. The conventional DWI and the SMS DWI with AF2 showed stable lesion conspicuity ([AF1/AF2]: reader 1 [1.8/1.4] and reader 2 [1.8/1.4]). The lesion conspicuity was lower using AF3 (reader 1: 2.2 and reader 2: 1.8). CONCLUSIONS In conclusion, SMS DWI of the kidney is a potential tool to substantially reduce scan time without negative effects on SNR, ADC quantification accuracy, and image quality if an AF2 is used. Although AF3 results in even higher scan time reduction, a negative impact on image quality, SNR, ADC quantification accuracy, and lesion conspicuity must be considered.

DOI: https://doi.org/10.1097/RLI.0000000000000323

Originally published at:
Kenkel, David; Barth, Borna K; Piccirelli, Marco; Filli, Lukas; Finkenstädt, Tim; Reiner, Cäcilia S; Boss, Andreas (2017). Simultaneous multislice diffusion-weighted imaging of the kidney: a systematic analysis of image quality. Investigative Radiology, 52(3):163-169.
DOI: https://doi.org/10.1097/RLI.0000000000000323

Simultaneous Multislice Diffusion-Weighted Imaging of the Kidney
A Systematic Analysis of Image Quality

David Kenkel, MD, Borna K. Barth, MD,* Marco Piccirelli, PhD,† Lukas Filli, MD,* Tim Finkenstädt, MD,* Cäcilia S. Reiner, MD,* and Andreas Boss, MD, PhD**

Objectives: The aims of this study were to implement a protocol for simultaneous multislice (SMS) accelerated diffusion-weighted imaging (DWI) of the kidneys and to perform a systematic analysis of image quality of the data sets.

Materials and Methods: Ten healthy subjects and 5 patients with renal masses underwent DWI of the kidney in this prospective institutional review board–approved study on a 3 T magnetic resonance scanner. Simultaneous multislice DWI echo-planar sequences (acceleration factors [AFs] 2 and 3) were compared with conventional echo-planar DWI as reference standard for each acquisition scheme. The following 3 acquisition schemes were applied: comparison A, with increased number of acquisitions at constant scan time; comparison B, with reduction of acquisition time; and comparison C, with increased slice resolution (constant acquisition time, increasing number of slices). Interreader reliability was analyzed by calculating the intraclass correlation coefficient (ICC). Qualitative image quality features were evaluated by 2 independent radiologists on a 5-point Likert scale. Quantification accuracy of the apparent diffusion coefficients (ADCs) and signal-to-noise ratios (SNRs) were assessed by region of interest analysis. Furthermore, lesion conspicuity in the 5 patients was assessed using a 5-point Likert scale by 2 independent radiologists.

Results: Interreader agreement was substantial with an ICC of 0.68 for the overall image quality and an ICC of 0.73 for the analysis of artifacts. In comparison A, AF2 resulted in increased SNR ($P < 0.05$) by 21% at stable image quality scores (image quality: $P = 0.76$, artifacts: $P = 0.21$). In comparison B, applying AF2, the scan time could be reduced by 46% without significant reduction in qualitative image quality scores ($P = 0.059$) or SNR ($P = 0.126$). In comparison C, slice resolution could be improved by 28% using AF2 with stable image quality scores and SNR. In general, AF3 resulted in reduced image quality and SNR. Significantly reduced ADC values were observed for AF3 in comparison C (cortex: $P = 0.003$; medulla: $P = 0.001$) compared with the standard echo-planar imaging sequence. The conventional DWI and the SMS DWI with AF2 showed stable lesion conspicuity ([AF1/AF2]: reader 1 [1.8/1.4] and reader 2 [1.8/1.4]). The lesion conspicuity was lower using AF3 (reader 1: 2.2 and reader 2: 1.8).

Conclusions: In conclusion, SMS DWI of the kidney is a potential tool to substantially reduce scan time without negative effects on SNR, ADC quantification accuracy, and image quality if an AF2 is used. Although AF3 results in even higher scan time reduction, a negative impact on image quality, SNR, ADC quantification accuracy, and lesion conspicuity must be considered.

Key Words: simultaneous multislice, diffusion-weighted imaging, DWI, kidney, image quality

(*Invest Radiol* 2016;00: 00–00)

Diseases of the kidney are a common reason for hospitalization and ambulant treatment. Chronic kidney disease (CKD) was ranked as 18th most important cause of death in 2010 with an increasing tendency over the last decades,[1] and currently, more than 2 million people receive treatment worldwide.[2] Furthermore, kidney cancer is with 338,000 new cases diagnosed in 2012, the 12th most common cancer worldwide.[3]

Diffusion-weighted imaging (DWI) is a potent diagnostic tool for the assessment of a variety of kidney pathologies; DWI allows the early detection of dysfunction in renal allografts[4] and diabetic nephropathy.[5] Another field of application of DWI is the detection[6] and evaluation[7] of infections of the kidney, and DWI may be used for the assessment of the severity of CKD during the course of the disease.[8,9] Furthermore, DWI enables to characterize renal lesions,[10] including renal cell carcinoma subtypes,[11,12] and to distinguish among different types of solid renal tumors.[13] Nevertheless, the ability of DWI to differentiate between benign and malignant renal tumors, however, remains controversial.[12,14,15] Although DWI bears this broad variety of potential applications, it is not yet part of most clinical routine protocols, which might be caused mainly by 2 reasons: first, the lack of standardization of DWI acquisitions and the consecutive difficulty of the differentiation of benign and malignant renal lesions based on apparent diffusion coefficient (ADC) values and, second, the relatively long acquisition time.

Recent advances in magnetic resonance imaging (MRI) techniques such as simultaneous multislice (SMS) diffusion imaging, also known as multiband or slice-accelerated MRI, might contribute to the application of DWI in the clinical routine because it bears the potential to drastically reduce scan time. The fundamental idea behind slice-accelerated imaging is to simultaneously excite multiple slice planes at once. Because these slices would otherwise show aliasing, sophisticated readout techniques such as CAIPIRINHA (controlled aliasing in parallel imaging results in higher acceleration)[16,17] and a blip strategy according to Setsompop et al[18] have to be applied.

Up to date, for the kidney, a systematic analysis of image quality and acquisition parameters using an SMS DWI sequence has not been performed. The objective of this study was to optimize a kidney DWI protocol using an SMS sequence with different acceleration factors (AFs) for (*a*) improved signal-to-noise ratio (SNR) at identical scan time, (*b*) shorter acquisition time, or (*c*) higher slice resolution at identical scan time and to evaluate the different acquisition protocols regarding image quality, available SNR, and quantitative ADC differences.

MATERIALS AND METHODS

Study Population

In this institutional review board–approved study, 10 healthy subjects (6 men and 4 women) were prospectively examined. The mean age was 30.8 ± 7.4 years and ranged between 25 and 50 years. In average, the participants had a weight of 72.4 ± 15.7 kg (range, 54–105 kg) and a height of 177 ± 11.8 cm (range, 158–200 cm). The study was approved by the local ethics committee, and all volunteers gave written informed consent for the measurements and the evaluation of the acquired data. Moreover, 5 patients were evaluated in this study including 3 patients with simple cysts and 2 patients with solid enhancing masses under active surveillance (differential diagnosis: renal cell carcinoma; differential diagnosis: oncocytoma). Patients did not report discomfort due to accelerated sequences.

Received for publication June 27, 2016; and accepted for publication, after revision, August 11, 2016.

From the Departments of *Diagnostic and Interventional Radiology, and †Neuroradiology, University Hospital Zurich, Switzerland.

Conflicts of interest and sources of funding: none declared.

Correspondence to: David Kenkel, MD, Department of Diagnostic and Interventional Radiology, University Hospital Zurich, University of Zurich, Ramistrasse 100, CH-8091 Zurich, Switzerland. E-mail: david.kenkel@usz.ch.

ISSN: 0020-9996/16/0000–0000
DOI: 10.1097/RLI.0000000000000323

TABLE 1. Summary of All Scan Parameters

Scan Parameter	Sequence a1	Sequence a2	Sequence a3	Sequence b1/c1	Sequence b2	Sequence b3	Sequence c2	Sequence c3
Echo time, ms	65	65	65	65	65	65	65	65
Repetition time, ms	7.200	3.700	2400	6.600	3.300	2.400	4.200	3.600
FoV read, mm	400	400	400	400	400	400	400	400
FoV phase, %	78.1	78.1	78.1	78.1	78.1	78.1	78.1	78.1
In-plane resolution, mm^2	2.1 × 2.1	2.1 × 2.1	2.1 × 2.1	2.1 × 2.1	2.1 × 2.1	2.1 × 2.1	2.1 × 2.1	2.1 × 2.1
Slice thickness, mm	5	5	5	5	5	5	4	3
No. slices	42	42	45	42	42	45	54	69
Bandwidth, Hz/px	1736	1736	1736	1736	1736	1736	1736	1736
Fat saturation	SPAIR	SPAIR	SPAIR	SPAIR	SPAIR	SPAIR	SPAIR	SPAIR
Shim	Standard	Standard	Standard	Standard	Standard	Standard	Standard	Standard
In-plane parallel imaging	GRAPPA 2	GRAPPA 2	GRAPPA 2	GRAPPA 2	GRAPPA 2	GRAPPA 2	GRAPPA 2	GRAPPA 2
Slice acceleration	—	Factor 2	Factor 3	—	Factor 2	Factor 3	Factor 2	Factor 3
Diffusion mode	3-scan trace	3-scan trace	3-scan trace	3-scan trace	3-scan trace	3-scan trace	3-scan trace	3-scan trace
b-values (averages), s/mm^2	0 (1); 50 (1) 400; (2); 800 (4)	0 (2); 50 (2) 400; (4); 800 (8)	0 (2); 50 (3) 400; (6); 800 (12)	0 (2); 50 (2) 400; (4); 800 (8)	0 (2); 50 (2) 400; (4); 800 (8)	0 (2); 50 (2) 400; (4); 800 (8)	0 (3); 50 (3) 400; (6); 800 (12)	0 (4); 50 (4) 400; (8); 800 (16)
Acquisition time, min:s	3:14	3:13	3:15	5:23	2:55	2:14	5:15	5:59

Scan parameters for comparison A (sequence a1, a2, a3): different AF, constant scan time. Scan parameters for comparison B (sequence b1/c1, b2, b3): maximal reduction of acquisition time. Scan parameters for comparison C (sequence b1/c1, c2, c3): constant acquisition time, increasing number of slices, and decreasing slice thickness. The standard EPI sequences are highlighted in gray.

FoV indicates field of view; SPAIR, spectral attenuated inversion recovery; GRAPPA, generalized autocalibrating partially parallel acquisition.

Magnetic Resonance Imaging

All image data were acquired on a 3 T Siemens MRI scanner (MAGNETOM Skyra; Siemens Healthcare, Erlangen, Germany) equipped with parallel transmit technology. The sequences were applied in free breathing. The volunteers were scanned in supine position, and a 32-element spine matrix coil and an 18-element body matrix coil were used for signal reception.

The acquisition parameters of a single-shot spin-echo echo-planar imaging (EPI) sequence capable of SMS were optimized regarding the strategies mentioned hereafter; a conventional DWI EPI sequence was applied as reference standard. The SMS sequence used the previously published blipped CAIPIRINHA technique and the slice GRAPPA (generalized autocalibrating partially parallel acquisition) reconstruction technique.[16–18] The AF determined the number of simultaneously excited slices.

Three different sequence optimization schemes were applied to achieve:

A. Increase in SNR: by increase in AF, increase in number of averages, acquisition time constant;
B. Reduce acquisition time: by increase in AF; and
C. Increase slice resolution: by increase in AF and investing the time that is gained in a reduced slice thickness and increased number of slices, thereby improving spatial resolution and keeping SNR stable by increasing the number of averages.

Each optimization scheme was carried out for AF2 and AF3; moreover, a conventional DWI sequence was acquired as reference standard. Table 1 gives an overview of the acquisition parameters of the compared sequences. For all sequences, SPAIR (spectral attenuated inversion recovery) fat saturation was applied with previous standard automatic shimming.

Evaluation of Image Quality

Image quality of the DWI trace images of the high b-value (800 s/mm^2) was evaluated by 2 independent radiologists with 10 years

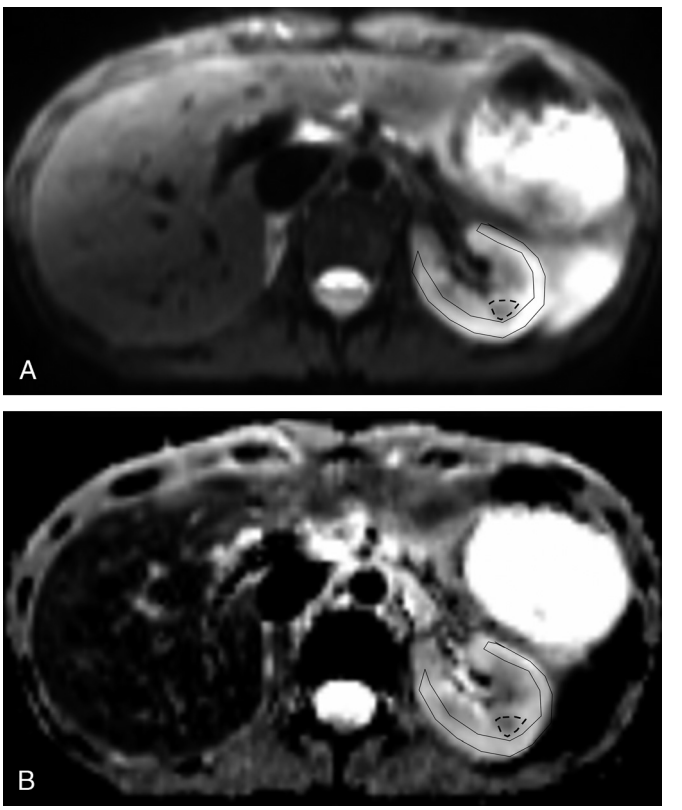

FIGURE 1. Typical ROI placement in the renal cortex and medulla is shown on the diffusion-weighted images with a b-value of 50 s/mm^2 (A) and on the corresponding ADC maps (B).

TABLE 2. Mean Values, Standard Deviations, and *P* Values of ADC Values From All Different Acquisition Protocols

Sequence	ADC Cortex ($\times 10^{-3}$ mm^2/s)	*P*: SMS vs Standard EPI	ADC Medulla ($\times 10^{-3}$ mm^2/s)	*P*: SMS vs Standard EPI
a1	2.08 ± 0.12		1.86 ± 0.11	
a2	2.06 ± 0.12	0.49	1.83 ± 0.11	0.23
a3	2.04 ± 0.12	0.28	1.84 ± 0.16	0.45
b1/c1	2.04 ± 0.09		1.84 ± 0.08	
b2	2.08 ± 0.15	0.18	1.84 ± 0.10	0.97
b3	2.00 ± 0.13	0.18	1.85 ± 0.13	0.85
c2	2.04 ± 0.11	0.84	1.84 ± 0.08	0.80
c3	1.96 ± 0.12	0.003	1.75 ± 0.12	0.001

ADC indicates apparent diffusion coefficient; SMS, simultaneous multislice; EPI, echo-planar imaging.

and 4 year of experience. A 5-point Likert scale was used to rate the occurrence of artifacts (1 indicates no artifacts; 2, mild artifacts; 3, moderate artifacts; 4, severe artifacts; and 5, not diagnostic) and the overall image quality (1 indicates excellent; 2, good, not affecting interpretation; 3, moderate, potentially affecting interpretation; 4, poor, definitely affecting interpretation; 5, not diagnostic). In addition, the frequency of artifacts was counted from the pooled data from both readers.

Furthermore, image quality was quantitatively assessed by calculating the SNR using the subtraction method.[19] Two stacks of images with identical scanning settings were acquired and subtracted thus generating a difference/noise image. The mean of the original images was used to measure the signal.[20] The regions of interest (ROIs) were placed in pars intermedia of the kidneys as shown in Figure 1. The mean ROI size in the cortex was 3.98 ± 1.27 cm^2 and that in the medulla was 0.77 ± 0.28 cm^2. In addition, the SNR per time was calculated by dividing the SNR by the acquisition time.

Quantitative ROI Analysis of ADC Values

To evaluate the comparability, ADC maps were automatically calculated by the sequence, and ADC values were measured using an ROI analysis of renal cortex and medulla. The ROIs were placed in pars intermedia of the kidneys as shown in Figure 1. The mean values and the standard deviations of the ADC values were calculated and compared with the literature values.

Statistical Analysis

Continuous variables were summarized by using means and standard deviations. Categorical variables were summarized as counts and proportions. The distribution of data was assessed with the Kolmogorov-Smirnov test. The SNR and ADC values were compared for every sequence using Mann-Whitney *U* test with Bonferroni correction for multiple comparisons. Furthermore, interreader reliability was analyzed by calculating the intraclass correlation coefficient (ICC). The interpretation of the ICC values was done according to Kundel and Polansky[21]: values of 0.81 to 1.00 indicate almost perfect; 0.61 to 0.80, substantial; 0.41 to 0.60, moderate; 0.21 to 0.40, fair; and less than 0.20, poor agreement. Statistical analysis was performed with the SPSS 22.0 software package (IBM SPSS Statistics, version 22, IBM Corp, Somers, NY). A *P* value of less than 0.05 was considered significant.

Initial Experience With Lesion Conspicuity

Lesions were assessed on the ADC map by 2 independent radiologists with 10 years and 4 year of experience on a 5-point Likert-scale (1 indicates excellent conspicuity compared with surrounding tissue; 2, good conspicuity compared with surrounding tissue, not affecting interpretation; 3, moderate conspicuity compared with surrounding tissue, potentially affecting interpretation; 4, faint conspicuity

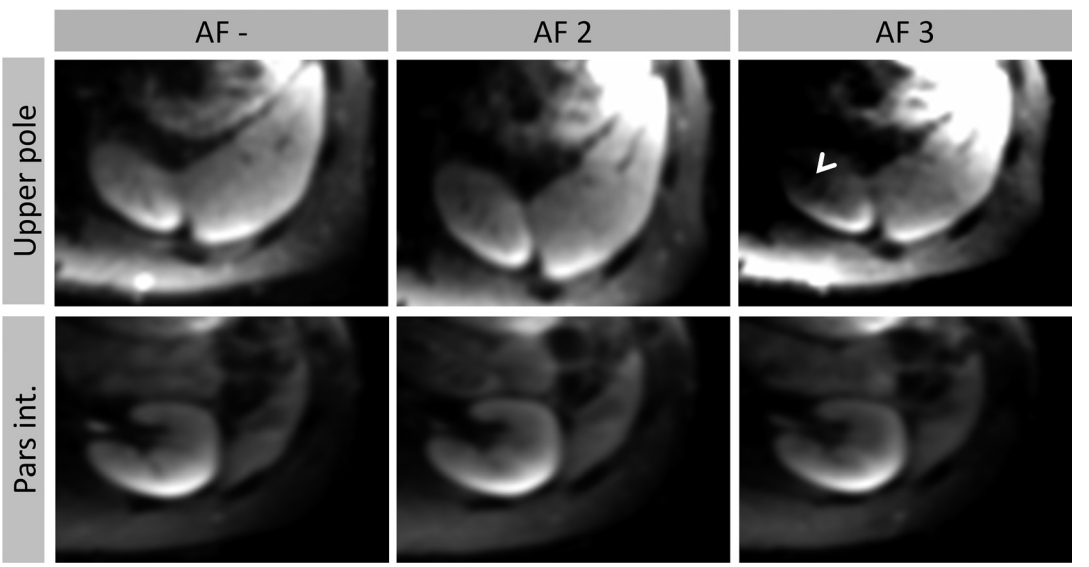

FIGURE 2. Typical examples of images acquired with different AF are displayed. In addition, a typical artifact with decreased signal intensity in the upper kidney pole caused by slice acceleration (AF3, white arrow) is shown. In pars intermedia, no such artifact can be observed.

TABLE 3. Results of the SNR and Image Quality Analysis

Sequence	Image Quality	Artifacts	No. Artifacts (n)	SNR
Comparison A: different AF, constant scan time				
Sequence a1, AF1, averages 1/2/4	2.00 ± 0.73	1.60 ± 0.88	0	15.6 ± 2.2
Sequence a2, AF2, averages 2/4/8	1.80 ± 0.83	1.65 ± 0.93	0	18.9 ± 2.9
Sequence a3, AF3, averages 3/6/12	2.25 ± 0.91	1.95 ± 1.05	2	15.6 ± 3.2
Comparison B: maximal reduction of acquisition time				
Sequence b1/c1, AF1, AT 5:23 min	1.63 ± 0.90	1.42 ± 0.77	1	20.3 ± 3.3
Sequence b2, AF2, AT 2:55 min	1.90 ± 0.97	1.55 ± 0.69	1	18.8 ± 3.6
Sequence b3, AF3; AT 2:14 min	2.50 ± 0.83	2.10 ± 0.91	1	15.9 ± 3.7
Comparison C: constant acquisition time, increasing no. slices, and decreasing slice thickness				
Sequence b1/c1, AF1, ST 5 mm	1.63 ± 0.90	1.42 ± 0.77	1	20.3 ± 3.3
Sequence c2, AF2, ST 4 mm	1.68 ± 0.75	1.53 ± 0.77	2	20.1 ± 3.6
Sequence c3, AF3, ST 3 mm	2.55 ± 0.83	2.55 ± 0.94	1	18.4 ± 4.5

The mean and standard deviation are shown for all sequences.

SNR indicates signal-to-noise ratio; AF, acceleration factor.

compared with surrounding tissue, definitely affecting interpretation; and 5, lesion cannot be differentiated from surrounding tissue).

RESULTS

Data were acquired for all volunteers successfully, and no data set had to be excluded. As an incidental finding of the anatomical analysis, 1 subject exhibited atrophy of the left lower pole of the kidney. In general, quantitative analysis showed mean ADC values that ranged from 1.96 ± 0.12 ($\times 10^{-3}$ mm^2/s) to 2.08 ± 0.12 ($\times 10^{-3}$ mm^2/s) for the renal cortex and 1.75 ± 0.12 ($\times 10^{-3}$ mm^2/s) to 1.86 ± 0.11 ($\times 10^{-3}$ mm^2/s) for renal medulla. Table 2 gives an overview of the mean ADC values of renal cortex and medulla for all sequences. Interreader agreement for all sequences was substantial with an ICC of 0.68 for the overall image quality and an ICC of 0.73 for the analysis of artifacts. Figure 2 shows examples of image acquisitions also depicting a typical artifact with decreased signal intensity in the upper kidney pole caused by slice acceleration.

Comparison A: Different AF, Increased Averages, Constant Acquisition Time

Table 3 gives an overview of the qualitative and quantitative evaluation of image quality, and Figure 3 depicts the results of comparison A. The SMS sequences a2 and a3 showed no significant difference in the presence of artifacts and in the overall image quality compared with the standard sequence a1. Signal-to-noise ratio was significantly higher using an AF2 ($P = 0.002$), whereas the SNR of the SMS sequence with AF3 and the standard sequence was similar ($P = 0.13$).

Comparison B: Maximal Reduction of Acquisition Time

Only the sequence using an AF3 showed a significant degradation of image quality in the reader scores compared with the standard sequence (artifacts: $P = 0.003$; image quality: $P = 0.003$), whereas the AF2 sequence (b2) exhibited stable reader scores. The SMS sequence with AF2 (b2) exhibited similar SNR compared with the reference sequence (b1), whereas the sequence with AF3 (b3) had a significantly lower SNR compared with the standard sequence ($P = 0.002$). The SNR/time for sequence b1/c1 was 3.77/min, for sequence b2 6.44/min (increase by 70.8%), and for sequence b3 7.13/min (increase by 89.1%). Table 3 gives an overview of the qualitative and quantitative evaluation of image quality, and Figure 4 depicts the results of comparison B.

Comparison C: Constant Acquisition Time, Increasing Number of Slices, and Decreasing Slice Thickness

The image quality scores showed a significantly reduced image quality using the slice AF3 (artifacts: $P = 0.006$; image quality:

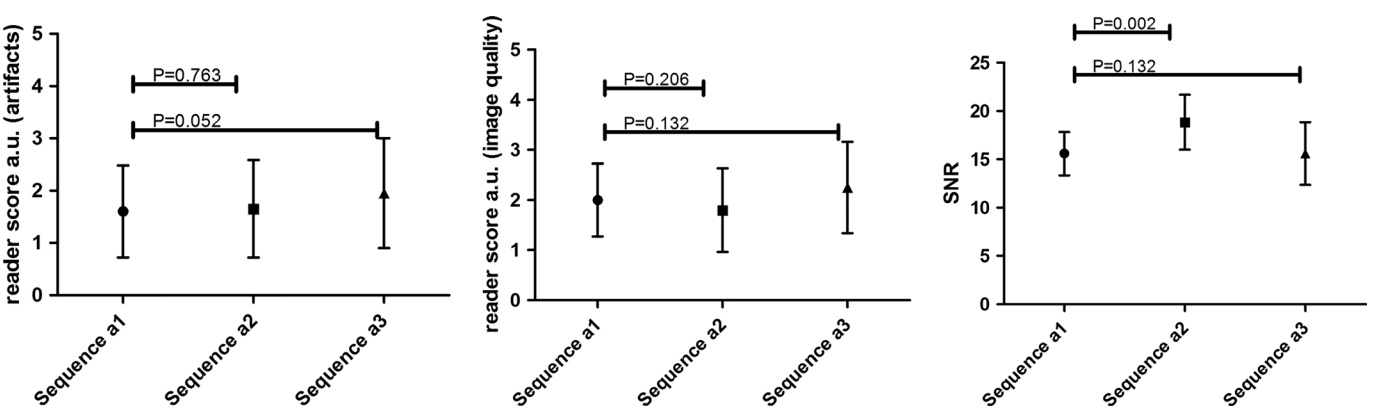

FIGURE 3. Comparison A (different AF, increased averages, constant acquisition time): depiction of the mean of image quality scores (arbitrarily units), SNR, and effect of artifacts. In general, a score of 1 means best image quality; a value of 5 means worst image quality. Error bars indicate standard deviation; a.u. indicates arbitrarily units.

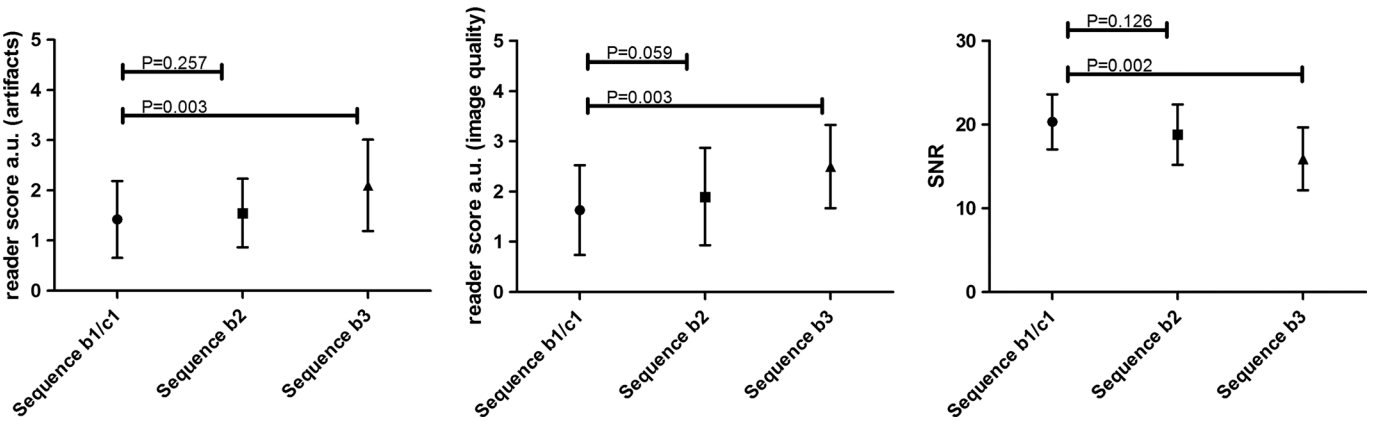

FIGURE 4. Comparison B (maximal reduction of acquisition time): depiction of the mean of image quality scores, SNR, and effect of artifacts. In general, a score of 1 means best image quality; a value of 5 means worst image quality. Error bars indicate standard deviation; a.u. indicates arbitrarily units.

$P = 0.003$). Comparing the SMS sequences and the standard sequence, no significant differences were observed in SNR values. A summary of the results of comparison C for the qualitative and quantitative evaluation of image quality is shown in Table 3 and Figure 5.

Frequency of Artifacts (Pooled Data From Both Readers)

The number of all acquired sequences for all volunteers in this study is 80 sequences (20 standard sequences and 60 SMS sequences). In 9/80 sequences, artifacts were observed that affected the depiction of the kidneys, which in all cases was a reduction of the signal in the upper pole of the kidney. The presence of relevant artifacts (artifact score ≥ 3) is shown in Table 3. The majority of artifacts were observed on SMS sequences: 8 of the 9 sequences showing artifacts were SMS sequences and one a standard sequence.

Initial Experience With Lesion Conspicuity

Table 4 shows the results of the readout of the lesion conspicuity of different renal lesions. While the conventional DWI and the SMS DWI with AF2 showed the same lesion conspicuity ([AF1/AF2]: reader 1 [1.8/1.4] and reader 2 [1.8/1.4]), the lesion conspicuity in contrast was lower using AF3 (reader 1: 2.2 and reader 2: 1.8). Figure 6 shows an example of a solid renal mass (patient 2) with decreased lesion conspicuity with a decreased area of diffusion restriction on the image acquired with AF3.

DISCUSSION

Several studies have shown the benefit of SMS DWI for different tissues such as the breast,[22] the skeletal muscle,[19] and the liver.[23–25] This is the first study assessing the image quality of SMS DWI for the depiction of the kidney.

In this study, the effects of different acquisition parameters on the image quality for SMS DWI of the kidneys were systematically analyzed. We showed that SMS DWI sequences can be used to (1) increase the SNR (comparison A) at constant scan time using an AF2/increased averages, (2) decrease scan time with temporal SNR efficiency (comparison B) thereby preserving comparable image quality using an AF2, and (3) increase slice resolution (comparison C) at constant scan time applying an AF2. At the moment, AF3 results in a substantially reduced image quality in all acquisition schemes. Comparing our results on ADC quantification to previous studies on DWI measurements of the kidneys,[4,5,10,11,13,15,26–31] the obtained ADC values are in line with reported data (compare Table 5) mostly in the lower range of the published ADC values. In our study, we showed that SMS can cause lower ADC values compared with standard sequences when an AF3 is chosen. Therefore, when comparing renal ADC values, this effect must be taken into account either by only comparing ADC values from

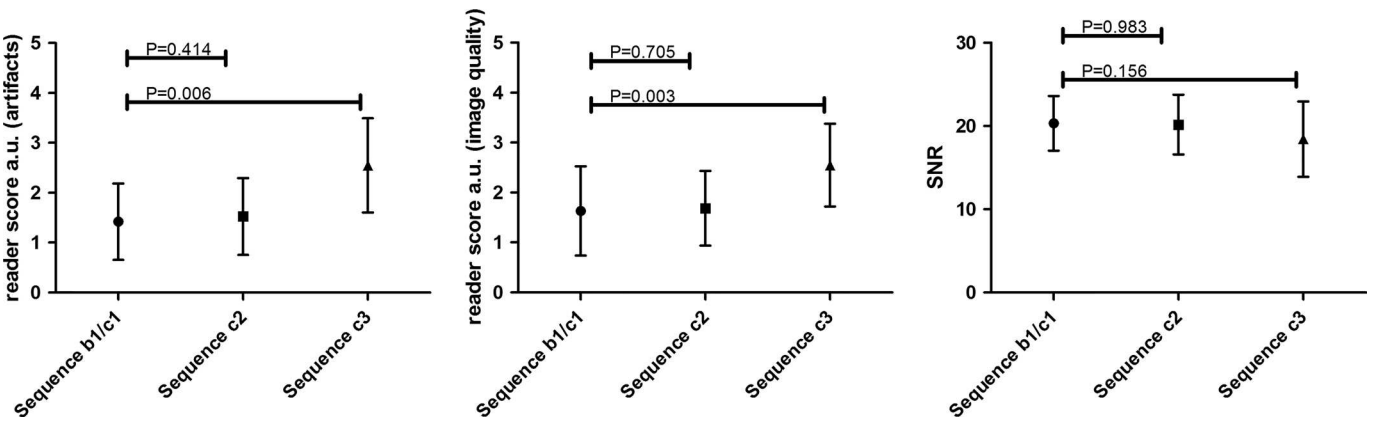

FIGURE 5. Comparison C (constant acquisition time, increasing number of slices, and decreasing slice thickness): depiction of the mean of image quality scores, SNR, and effect of artifacts. In general, a score of 1 means best image quality; a value of 5 means worst image quality. Error bars indicate standard deviation; a.u. indicates arbitrarily units.

TABLE 4. Lesion Conspicuity of Different Renal Lesions in 5 Patients

	ADC					
	AF1		AF2		AF3	
Patient Number (Type of Lesion)	Reader 1	Reader 2	Reader 1	Reader 2	Reader 1	Reader 2
Patient 1 (RCC/oncocytoma)	3	2	3	2	3	2
Patient 2 (RCC/oncocytoma)	1	1	1	1	2	1
Patient 3 (simple cyst)	1	1	1	1	1	1
Patient 4 (simple cyst)	2	1	2	1	2	2
Patient 5 (simple cyst)	2	2	2	2	3	3
Mean (SD)	1.8 (0.84)	1.4 (0.55)	1.8 (0.84)	1.4 (0.55)	2.2 (0.84)	1.8 (0.84)

Five-point Likert scale: 1 indicates excellent conspicuity compared with surrounding tissue; 2, good conspicuity compared with surrounding tissue, not affecting interpretation; 3, moderate conspicuity compared with surrounding tissue, potentially affecting interpretation; 4, faint conspicuity compared with surrounding tissue, definitely affecting interpretation; and 5, lesion cannot be differentiated from surrounding tissue.

ADC indicates apparent diffusion coefficient; RCC, renal cell carcinoma.

sequences with identical AF (eg, within the same institution) or by applying a respective correction factor to the data. This finding is substantial for the clinical applicability of SMS DWI because different pathologies might have different thresholds depending on the preexisting illnesses of the patient (eg, diabetic nephropathy[5] or severity of CKD[8,9]). However, this assumption needs to be proven in further studies. In addition, a higher volume of the patient, for example, caused by ascites and obesity, would reduce SNR because the increased distance of inner organs from the receiver coils in obese patients reduces the signal. However, the extent of this effect on SNR and the consecutive impact on diagnostic accuracy at different AF remain to be further investigated.

Furthermore, our findings concerning the SNR/time are in accordance with previous studies evaluating SMS DWI in other organs: with an AF2 in muscle of 50% to 60%[19] and in breast tissue of 61%[22] increase in SNR/time (our study 70.8%) and with an AF3 in muscle of 80% to 90%[19] and in breast tissue of 104%[22] increase in SNR/time (our study 89.1%).

Despite the even higher SNR/time that an AF3 offers compared with AF2, the resulting artifacts render the image quality nondiagnostic. In general, the sequence would even allow for AF4, which we, however, did not evaluate due to the little likelihood of a beneficial outcome. At the moment, we consider an AF2 to be the best compromise between ADC quantification accuracy, scan time, and image quality. However, we assume that—due to the rapid progress in the development of SMS sequences—soon even higher AF will become feasible. It must be pointed out that an increase of nearly 100% of SNR/time using an AF3 corresponds to the change from 1.5 T to 3.0 T magnetic field strength. This increase in field strength initially resulted in numerous challenges with artifacts due to B0 field inhomogeneity, higher specific absorption rates, and B1 interferences, which however mostly have been resolved within recent years.

The reduced scan time might be helpful for diffusion schemes that are known to have long acquisition times such as intravoxel incoherent motion[34] or diffusion tensor imaging, for example, whole-body applications.[35] Furthermore, the reduced scan time might be used for respiratory triggering, potentially improving image quality compared with shallow breathing.

There are some limitations to our study. First, this study was performed on a 3 T MR scanner only, and no comparison to a 1.5 T or 7 T MR scanner was performed and, therefore, the image quality at other field strength remains unknown. Setsompop et al[18] could show that the unaliasing of simultaneously acquired slices might be better at 7 T. Furthermore, it is known that susceptibility artifacts decrease at lower field strength; therefore, SMS DWI at 1.5 T presumably exhibits even less artifacts.

Second, the main objective of our study was to assess the image quality of SMS DWI in the kidney of healthy volunteers. Further, we

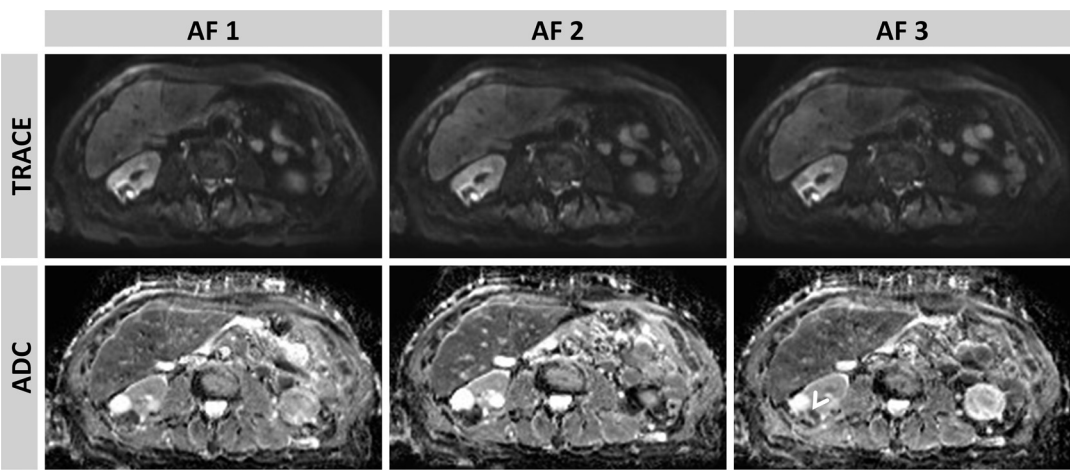

FIGURE 6. Example of a solid renal mass (patient 2): ADC map shows decreased lesion conspicuity with a decreased area of diffusion restriction on the image acquired with an AF3.

TABLE 5. Range of ADC Values of Our Study and the Literature Values of ADC Values of Renal Cortex and Medulla

Study	ADC Renal Cortex ($\times 10^{-3}$ mm^2/s)	ADC Renal Medulla ($\times 10^{-3}$ mm^2/s)
Kiliçkesmez et al[32]	2.08 ± 0.22	1.94 ± 0.18
Chow et al[33]	2.58 ± 0. 53	2.09 ± 0.55
Park et al[4]	2.10 ± 0.12	1.99 ± 0.14
Suo et al[26]	2.17 ± 0.14 to 2.38 ± 0.19	1.99 ± 0.16 to 2.20 ± 0.17
This study	1.96 ± 0.12 to 2.08 ± 0.12	1.75 ± 0.12 to 1.86 ± 0.11

ADC indicates apparent diffusion coefficient.

assessed lesion conspicuity in a limited number of patients with different renal lesions. Although we could show with our initial experiences that lesion conspicuity tends to be lower at AF3 and AF2 showed stable lesion conspicuity compared with conventional DWI, further studies are needed to assess the value of DWI for different pathologies.

In conclusion, SMS DWI of the kidney is a potential tool to reduce the scan time or increase slice resolution without negative effects on SNR, ADC quantification accuracy, and image quality, if moderate slice acceleration with AF2 is applied. Moreover, it might be used to slightly increase SNR at constant scan time. Although AF3 results in an even higher reduction in scan time, it exhibits a negative impact on SNR, ADC quantification, and image quality and thus potentially affecting lesion conspicuity.

REFERENCES

1. Jha V, Garcia-Garcia G, Iseki K, et al. Chronic kidney disease: global dimension and perspectives. *Lancet*. 2013;382:260–272.
2. Couser WG, Remuzzi G, Mendis S, et al. The contribution of chronic kidney disease to the global burden of major noncommunicable diseases. *Kidney Int*. 2011; 80:1258–1270.
3. Ferlay J, Soerjomataram I, Dikshit R, et al. Cancer incidence and mortality worldwide: sources, methods and major patterns in GLOBOCAN 2012. *Int J Cancer*. 136:E359–E386.
4. Park SY, Kim CK, Park BK, et al. Assessment of early renal allograft dysfunction with blood oxygenation level-dependent MRI and diffusion-weighted imaging. *Eur J Radiol*. 2014;83:2114–2121.
5. Chen X, Xiao W, Li X, et al. In vivo evaluation of renal function using diffusion weighted imaging and diffusion tensor imaging in type 2 diabetics with normoalbuminuria versus microalbuminuria. *Front Med*. 2014;8:471–476.
6. Henninger B, Reichert M, Haneder S, et al. Value of diffusion-weighted MR imaging for the detection of nephritis. *ScientificWorldJournal*. 2013;2013:8.
7. Chan JH, Tsui EY, Luk SH, et al. MR diffusion-weighted imaging of kidney: differentiation between hydronephrosis and pyonephrosis. *Clin Imaging*. 2001;25: 110–113.
8. Li Q, Li J, Zhang L, et al. Diffusion-weighted imaging in assessing renal pathology of chronic kidney disease: a preliminary clinical study. *Eur J Radiol*. 2014; 83:756–762.
9. Xu Y, Wang X, Jiang X. Relationship between the renal apparent diffusion coefficient and glomerular filtration rate: preliminary experience. *J Magn Reson Imaging*. 2007;26:678–681.
10. Mytsyk Y, Borys Y, Komnatska I, et al. Value of the diffusion-weighted MRI in the differential diagnostics of malignant and benign kidney neoplasms—our clinical experience. *Pol J Radiol*. 2014;79:290–295.
11. Choi YA, Kim CK, Park SY, et al. Subtype differentiation of renal cell carcinoma using diffusion-weighted and blood oxygenation level–dependent MRI. *Am J Roentgenol*. 2014;203:W78–W84.
12. Sevcenco S, Heinz-Peer G, Ponhold L, et al. Utility and limitations of 3-Tesla diffusion-weighted magnetic resonance imaging for differentiation of renal tumors. *Eur J Radiol*. 2014;83:909–913.
13. Sasamori H, Saiki M, Suyama J, et al. Utility of apparent diffusion coefficients in the evaluation of solid renal tumors at 3T. *Magn Reson Med Sci*. 2014;13:89–95.
14. Lassel EA, Rao R, Schwenke C, et al. Diffusion-weighted imaging of focal renal lesions: a meta-analysis. *Eur Radiol*. 2014;24:241–249.
15. Inci E, Hocaoglu E, Aydin S, et al. Diffusion-weighted magnetic resonance imaging in evaluation of primary solid and cystic renal masses using the Bosniak classification. *Eur J Radiol*. 2012;81:815–820.
16. Glover G. Phase-offset multiplanar (POMP) volume imaging: a new technique. *J Magn Reson Imaging*. 1991;1:457–461.
17. Breuer FA, Blaimer M, Heidemann RM, et al. Controlled aliasing in parallel imaging results in higher acceleration (CAIPIRINHA) for multislice imaging. *Magn Reson Med*. 2005;53:684–691.
18. Setsompop K, Gagoski BA, Polimeni JR, et al. Blipped-controlled aliasing in parallel imaging for simultaneous multislice echo planar imaging with reduced g-factor penalty. *Magn Reson Med*. 2012;67:1210–1224.
19. Filli L, Piccirelli M, Kenkel D, et al. Simultaneous multislice echo planar imaging with blipped controlled aliasing in parallel imaging results in higher acceleration: a promising technique for accelerated diffusion tensor imaging of skeletal muscle. *Invest Radiol*. 2015;50:456–463.
20. Goerner FL, Clarke GD. Measuring signal-to-noise ratio in partially parallel imaging MRI. *Med Phys*. 2011;38:5049–5057.
21. Kundel HL, Polansky M. Measurement of observer agreement. *Radiology*. 2003; 228:303–308.
22. Filli L, Ghafoor S, Kenkel D, et al. Simultaneous multi-slice readout-segmented echo planar imaging for accelerated diffusion-weighted imaging of the breast. *Eur J Radiol*. 2016;85:274–278.
23. Obele CC, Glielmi C, Ream J, et al. Simultaneous multislice accelerated free-breathing diffusion-weighted imaging of the liver at 3T. *Abdom Imaging*. 2015; 40:2323–2330.
24. Taron J, Martirosian P, Schwenzer NF, et al. Scan time minimization in hepatic diffusion-weighted imaging: evaluation of the simultaneous multislice acceleration technique with different acceleration factors and gradient preparation schemes. *MAGMA*. 2016;29:1–11.
25. Taron J, Martirosian P, Erb M, et al. Simultaneous multislice diffusion-weighted MRI of the liver: analysis of different breathing schemes in comparison to standard sequences. *J Magn Reson Imaging*. 2016. [Epub ahead of print].
26. Suo ST, Cao MQ, Ding YZ, et al. Apparent diffusion coefficient measurements of bilateral kidneys at 3 T MRI: effects of age, gender, and laterality in healthy adults. *Clin Radiol*. 2014;69:e491–e496.
27. Friedli I, Crowe LA, Viallon M, et al. Improvement of renal diffusion-weighted magnetic resonance imaging with readout-segmented echo-planar imaging at 3T. *Magn Reson Imaging*. 2015;33:701–708.
28. Wypych-Klunder K, Adamowicz A, Lemanowicz A, et al. Diffusion-weighted MR imaging of transplanted kidneys: preliminary report. *Pol J Radiol*. 2014: 94–98.
29. Kim B, Kim JH, Byun JH, et al. IgG4-related kidney disease: MRI findings with emphasis on the usefulness of diffusion-weighted imaging. *Eur J Radiol*. 2014;83: 1057–1062.
30. Kalayci TO, Apaydin M, Sönmezgöz F, et al. Diffusion-weighted magnetic resonance imaging findings of kidneys with obstructive uropathy: differentiation between benign and malignant etiology. *ScientificWorldJournal*. 2014;2014:5.
31. Bilgili MY. Reproductibility of apparent diffusion coefficients measurements in diffusion-weighted MRI of the abdomen with different b values. *Eur J Radiol*. 2012;81:2066–2068.
32. Kiliçkesmez O, Yirik G, Bayramoğlu S, et al. Non-breath-hold high b-value diffusion-weighted MRI with parallel imaging technique: apparent diffusion coefficient determination in normal abdominal organs. *Diagn Interv Radiol*. 2008;14: 83–87.
33. Chow LC, Bammer R, Moseley ME, et al. Single breath-hold diffusion-weighted imaging of the abdomen. *J Magn Reson Imaging*. 2003;18:377–382.
34. Wurnig MC, Donati OF, Ulbrich E, et al. Systematic analysis of the intravoxel incoherent motion threshold separating perfusion and diffusion effects: proposal of a standardized algorithm. *Magn Reson Med*. 2015;74:1414–1422.
35. Kenkel D, von Spiczak J, Wurnig MC, et al. Whole-body diffusion tensor imaging: a feasibility study. *J Comput Assist Tomogr*. 2016;40:183–188.